



Title	Host and guest joining forces : a holistic approach for metal-organic frameworks in nonlinear optics
Author(s)	Wolf, Mathias; Hirai, Kenji; Toyouchi, Shuichi; Daelemans, Brent; Fron, Eduard; Uji-i, Hiroshi
Citation	Journal of materials chemistry C, 10(25), 9471-9477 https://doi.org/10.1039/d2tc01075e
Issue Date	2022-07-07
Doc URL	http://hdl.handle.net/2115/90135
Type	article (author version)
File Information	JMaterChemC.pdf



[Instructions for use](#)

ARTICLE

Host and guest joining forces: a holistic approach for metal-organic frameworks in nonlinear optics†

Mathias Wolf,^a Kenji Hirai*,^b Shuichi Toyouchi,^c Brent Daelemans,^a Eduard Fron,^a Hiroshi Uji-i*^{a,b,d}

Received 00th January 20xx,
Accepted 00th January 20xx

DOI: 10.1039/x0xx00000x

Metal-organic frameworks (MOFs) are an interesting candidate for nonlinear optics (NLO) application. However, current design strategies for MOFs in NLO are typically limited to either engineering the MOF itself or using the MOF to align NLO-active molecules within its pores. But more design factors can be considered when engineering MOFs and choosing guest molecules. The NLO emission of host and guests can be combined instead of using only either one of the two. The interaction between host and guest can be source for further improvement by changing the symmetry, dipole moment, bond lengths, charge distribution, etc. Additionally, unstable NLO molecules can potentially be stabilized by accommodation in the MOF. Here, we demonstrate a new strategy for MOFs by combining MOF-177 as a host and Li@C₆₀ as guest for NLO meaning both the MOF itself as well as guest molecules are emitting NLO signal, as well as further increasing the emission using their interaction elongating bonds within the MOF, thus fully using the MOFs potential for second harmonic generation. Using this approach, the overall emission can be boosted by 40% compared to MOF-177 alone. Furthermore, the accommodation into MOF-177 stabilizes Li@C₆₀ that is normally unstable under ambient conditions without a counterion.

Introduction

Metal-organic frameworks (MOFs) have attracted great attention in applications such as gas storage and gas separation, catalysis or sensors due to their large surface area.¹⁻⁷ Recently, MOFs are further considered in an area of applications even larger than these primary fields. This is because their structure, consisting of metal ions and organic linkers, allows facile modification for various purposes by changing or modifying the linkers and/or metal nodes. In this way, many properties of MOFs can be tailor-made to suit exactly the intended application. Accommodation of metallofullerenes is an interesting way of further controlling the properties of MOFs and their accommodated guests.⁸⁻¹⁰

A more recent field for MOFs is nonlinear optics (NLO).¹¹⁻¹³ NLO has played a central role in modern photonics for a variety of applications ranging from laser frequency conversion, ultrafast information processing, sensors, switches, laser amplifiers etc.¹⁴⁻¹⁸ Current materials in NLO are often based on inorganic materials like salts and semiconductors.¹⁹ However, these materials have disadvantages like low optical damage threshold, being difficult and expensive to manufacture.²⁰ For this reason, there has been a push to use organic materials as they allow flexible design, good NLO properties and high

optical damage threshold.²⁰ MOFs as a class of inorganic-organic hybrids can combine the best of both worlds. A different strategy uses the ability of MOFs to accommodate NLO active molecules into their pores. Such a strategy can be viable for molecules that have strong NLO properties but poor crystallinity.

However, the combined emission of MOF and guest molecules has not been scrutinized so far. This means that either the pores of the MOF or the MOF itself are not efficiently used. Overall NLO performance could be enhanced if both NLO active MOF and guest are combined to obtain the desired emission. Furthermore, interaction between host and guest can further improve emission, *e.g.* by increasing the dipole moment or causing structural changes that increase non-centrosymmetry. Finally, accommodation in the MOF can potentially stabilize NLO-active molecules that would otherwise be unstable under ambient conditions or are difficult to crystallize with high quality. Considering all of these factors means fully taking advantage of the design flexibility of MOFs and organic compounds in general.

Here, we demonstrate how choosing suitable MOF and guest pair can significantly improve NLO emission and fully use the MOF volume. The guest molecule chosen in this study is lithium encapsulating C₆₀ (Li@C₆₀). It has been shown previously that Li@C₆₀ has superior NLO properties compared to ordinary C₆₀.²¹⁻²³ As Li@C₆₀ is a relatively large molecule, a MOF with large pores is necessary to accommodate it.²⁴⁻²⁶ For this reason, MOF-177 was chosen for its capability to accommodate C₆₀.^{8,9,27} Second-harmonic generation (SHG) can be increased by 40% by accommodating Li@C₆₀ into MOF-177. By additionally comparing the performance with C₆₀ accommodating MOF-177, we discuss the improvement of NLO emission by considering NLO of the guest molecule itself and the interaction between Li@C₆₀ and MOF-177.

^a Department of Chemistry, Celestijnenlaan 200F, 3001 Leuven, Belgium.

E-mail: hiroshi.uji@kuleuven.be

^b Research Institute for Electronic Science (RIES), Hokkaido University, N20W10, Kita ward, Sapporo, 001-0020 Hokkaido, Japan.

E-mail: hirai@es.hokudai.ac.jp

^c Department of Applied Chemistry, National Yang Ming Chiao Tung University, 1001 Ta Hsueh Rd., Hsinchu 30010, Taiwan.

^d Institute for Integrated Cell-Material Science (WPI-iCeMS), Kyoto University, Yoshida Sakyo-ku, Kyoto 606-8501, Japan

†Electronic Supplementary Information (ESI) available: [details of any supplementary information available should be included here]. See DOI: 10.1039/x0xx00000x

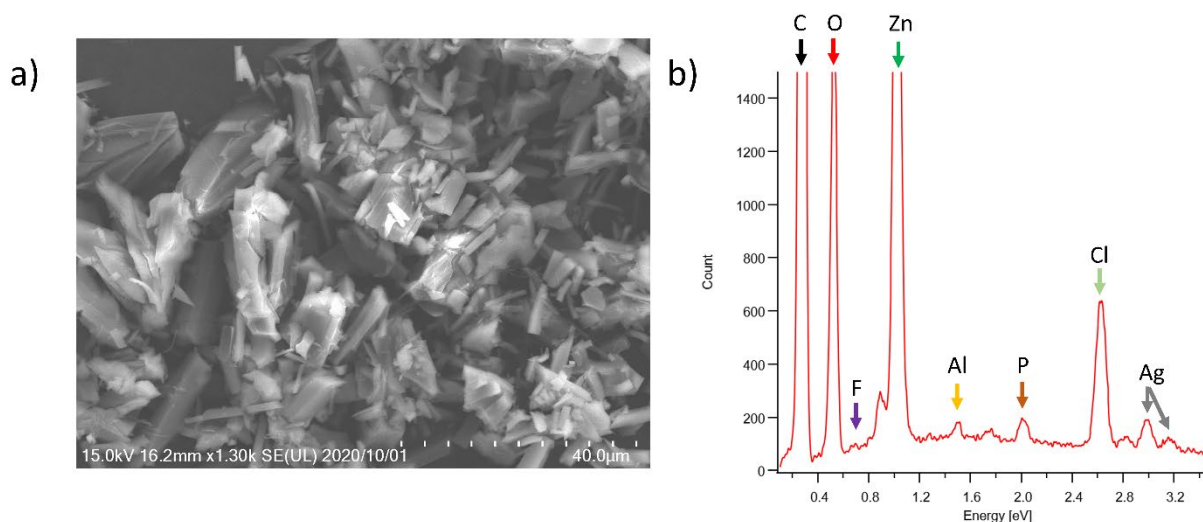


Fig. 1 a) SEM image of $\text{Li}@C_{60}/\text{MOF-177}$. b) EDX spectrum obtained. Only the small amounts of PF_6 are detected. Al is due to the sample holder, Ag is due to metal sputtering.

Results and discussion

Characterization of $\text{Li}@C_{60}/\text{MOF-177}$

$\text{Li}@C_{60}$ was accommodated into MOF-177 (Figure S1) by dissolving $\text{Li}^+@C_{60}(\text{PF}_6^-)$ powder in a 1:1 (v:v) mixture of *o*-dichlorobenzene (*o*DCB) and acetonitrile (ACN) (see experimental section for details). In order to explore the accommodation of $\text{Li}@C_{60}$ into MOF-177 more, we performed scanning electron microscopy (SEM) with energy dispersive X-ray (EDX) spectroscopy (see Figure 1). As can be seen from the EDX spectrum (Figure 1 b), there are only small amounts of phosphorus (P) and fluorine (F) present. In the powder of $\text{Li}^+@C_{60}(\text{PF}_6^-)$, PF_6^- is used as a counterion in order to balance the positive charge of Li^+ . It is known that $\text{Li}^+@C_{60}$ is not stable under ambient conditions unless paired with a counterion.²⁸ Therefore, the small amount of PF_6 indicates that another molecule, i.e. solvent molecules, or the MOF itself is serving as a counterion. It should be noted that chlorine (Cl) is present in the samples, meaning *o*DCB is co-accommodated. However, no nitrogen (N) that would point to ACN is detected.

We carried out attenuated total reflection measurement of Fourier-transform infrared spectroscopy (FT-IR) to further investigate the solvent molecules being accommodated. The results can be seen in Figure S2. FTIR shows the presence of both PF_6 and *o*DCB in $\text{Li}@C_{60}/\text{MOF-177}$, however no ACN is accommodated. Similarly, $C_{60}/\text{MOF-177}$ does show some amount of toluene accommodated.

Because Li is not detectable in EDX, inductively coupled plasma atomic emission spectroscopy (ICP-OES) was performed (Figure S3) showing a content of Li. The quantitative analyses of Li by ICP-OES is difficult because of the ionization interference of Li with Na (added in the solution to be pH7).²⁹ The chemical formula of $\text{Li}@C_{60}/\text{MOF-177}$ was estimated to be $\{\text{Zn}_4\text{O}(\text{btb})_2\} \cdot 0.3 \{[\text{Li}@C_{60}](\text{PF}_6)] \cdot (\text{oDCB})\}_n$ by

thermogravimetry (Figure S4, btb: benzene-1,3,5-tribenzoate). A single unit cell of MOF-177 ($[\text{Zn}_{32}\text{O}_8(\text{btb})_{16}]_n$) can accommodate 16 C_{60} molecules according to literature³⁰, meaning that 15 % of the available space is filled with $\text{Li}@C_{60}$. To further investigate the interaction of MOF-177 and $\text{Li}@C_{60}$, we have performed Raman spectroscopy (Figure 2). An interesting feature is the disappearance of the $A_g(2)$ mode, normally positioned at 1470 cm^{-1} and shifted slightly lower by 3 cm^{-1} in case of $\text{Li}@C_{60}[\text{PF}_6^-]$ powder²¹, after the accommodation into MOF-177 (Figure 2a, red highlighted and inset). This disappearance of the $A_g(2)$ mode cannot be seen after dissolving $\text{Li}@C_{60}$ in a mixture of ACN/*o*DCB (see Figure S5). This suggests that $\text{Li}@C_{60}$ is not interacting with either *o*DCB or ACN, despite it being co-accommodated, but actually with the MOF itself, suggesting the MOF could serve as a counterion. A similar change in the Raman spectrum cannot be seen when accommodating ordinary C_{60} into MOF-177 (see Figure S6). A similar vanishing of the $A_g(2)$ mode has been reported by Denisov *et al.* when studying superconducting films of K_3C_{60} and Rb_3C_{60} .³¹ When Raman was measured with 1064 nm laser excitation, no $A_g(2)$ mode could be observed, which has been attributed to a distortion of C_{60} due to the Jahn-Teller effect. For a better understanding of the interaction between MOF-177 and $\text{Li}@C_{60}$, a closer look at the Raman spectra, in particular at 415 cm^{-1} is useful. This peak originates from MOF-177 and can be attributed to the Zn-O bond vibration.^{32,33} Figure 2b shows the Raman peak for MOF-177 after soaking in the *o*DCB/ACN solution (black) and those with accommodated C_{60} (blue) and $\text{Li}@C_{60}$ (red), respectively. When $\text{Li}@C_{60}$ is accommodated, a peak shift to 412 cm^{-1} is observed, while such a shift was not observed for the other two, indicating that accommodation of $\text{Li}@C_{60}$ is the origin of this shift. Raman peaks shifting to lower frequencies is typically associated with strain in the system and in particular with tensile stress.³⁴ Similar shifts have been reported for phosphorus-oxide bonds as well as cobalt-doped Zn-O nanorods.^{35,36} This would indicate a lengthening of the Zn-O bonds in MOF-177. Likely, the positive charge of Li^+ is attracting oxygen and repelling zinc causing the bond length to

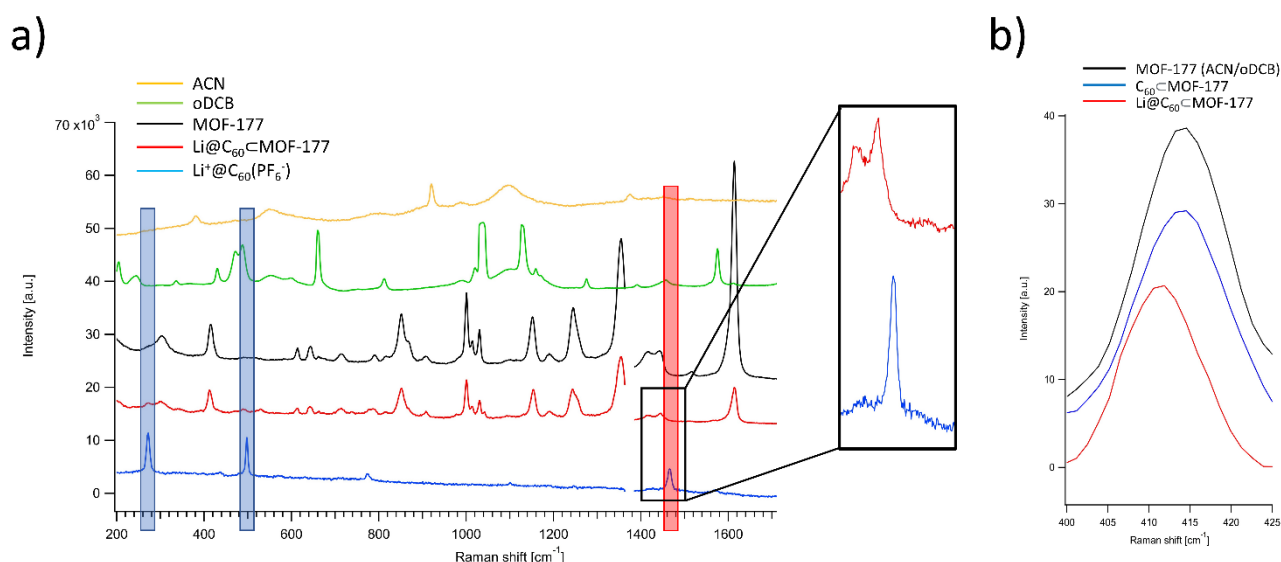


Fig. 2 a) Raman spectra of $\text{Li@C}_{60}[\text{PF}_6^-]$ (blue), $\text{Li@C}_{60}@$ MOF-177 (red) and MOF-177 (black) as well as oDCB (green) and ACN (yellow). The $A_g(2)$ mode peak of C_{60} is marked with a red square. It disappears after accommodation into MOF-177. Excitation wavelength was set to 785 nm. b) Close-up of the MOF-177 Raman peak resulting from the Zn-O bond. Shown are the spectra obtained from MOF-177 after storage in a 1:1 (v:v) oDCB/ACN solution (black), as well as with accommodated C_{60} (blue) and Li@C_{60} (red). A peak shift is observed only when Li@C_{60} is accommodated. Excitation wavelength was set to 633 nm. The spectra have been background-corrected, see Figure S7 for details.

increase. Similar interactions are causing the C_{60} cage in $\text{Li}^+@$ $\text{C}_{60}(\text{PF}_6^-)$ crystals to distort, as the nonpolar C_{60} repulses the Li^+ and/or PF_6^- . Similar forces in Li@C_{60} accommodating MOF-177 ($\text{Li@C}_{60}@$ MOF-177) could explain the above observed disappearance of the $A_g(2)$ mode of C_{60} as it can feel repulsive forces resulting from interaction with Li and O. Furthermore, the electrostatic interaction between Li@C_{60} and MOF-177 explain how Li@C_{60} can be stable without PF_6^- as a counterion. To investigate the homogeneity of C_{60} and Li@C_{60} in MOF-177, Raman scattering intensity mapping was carried out. C_{60} and Li@C_{60} were distributed in MOF-177 over several microns (Figures S8a-b). Additionally, C_{60} and Li@C_{60} were detected in the inner part of MOF-177 (Figures S8c-e). These results indicate that C_{60} and Li@C_{60} were encapsulated in the whole volume of MOF-177.

Nonlinear optical properties

In order to assess the NLO properties of the $\text{Li@C}_{60}@$ MOF-177 composite, we have performed SHG measurements under microscopy conditions. Figure 3 shows the average intensities of SHG obtained from MOF-177 (soaked in either toluene or a 1:1 (v:v) mixture of oDCB/ACN), C_{60} accommodating MOF-177 ($\text{C}_{60}@$ MOF-177) and $\text{Li@C}_{60}@$ MOF-177. As can be seen, the average emission after accommodation of Li@C_{60} has increased by roughly 40% compared to empty MOF-177 (soaked in toluene). This effect is not observed when C_{60} is accommodated. In fact, C_{60} shows only a marginal improvement that does not exceed standard deviation. MOF-177 soaked in oDCB/ACN also shows a substantial increase in emission, meaning the enhancement in $\text{Li@C}_{60}@$ MOF-177 is partially due to Li@C_{60} and partially due to oDCB. It should be mentioned that some part of the emitted SHG is likely re-absorbed by Li@C_{60} lowering the efficiency slightly (see Figure S9).

As SHG is a 2nd order NLO effect, it requires breaking of centrosymmetry in order to be observed. Due to this condition, it should be noted that MOF-177 originally has a centrosymmetric structure³⁷ and thus the emission of 2nd order NLO effects is not obvious. To check if this signal was not produced by the solvent molecules, we exposed MOF-177 to a vacuum for 30 minutes and performed NLO measurements. Indeed, SHG was clearly observed (see Figure S10). We can safely conclude that the signal is generated in the MOF itself (no signal could be observed from the coverslip). MOFs are known to have a soft structure due to their organic linkers meaning the linkers can e.g. rotate, which could cause the breakdown of

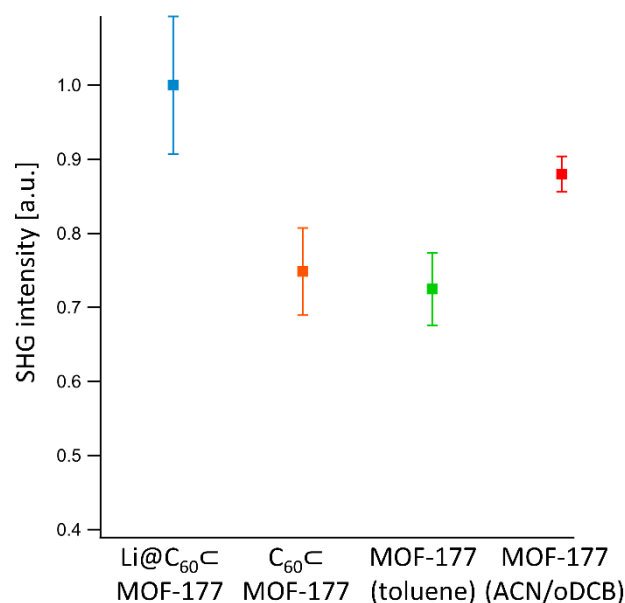


Fig. 3 Average maximum intensity obtained from different types of MOF-177 with standard deviations. Averages were obtained from 40 spectra for each type. SHG was excited using 820 nm irradiation with a pulse duration of 120 fs and a repetition rate of 80 MHz.

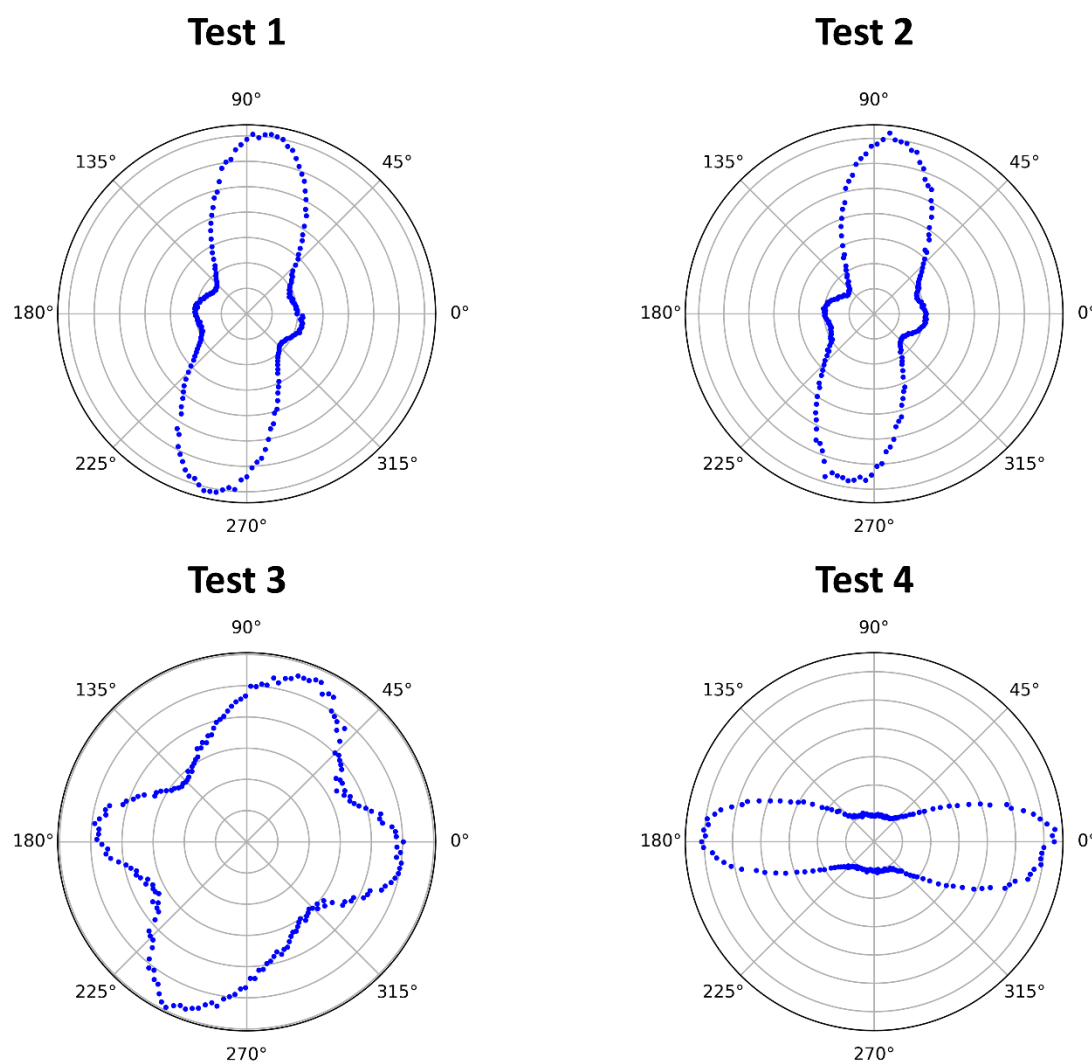


Fig. 4 Polarized SHG analysis performed on MOF-177. Test 1: a linear polarized pulsed beam is rotated 360° and all emitted SHG collected. Test 2: the beam is rotated 360° and the emitted SHG measured with an arbitrary polarization using an analyzer. Test 3: the beam polarization and analyzer are rotated 360° in parallel. Test 4: the beam polarization and analyzer are rotated 360° but perpendicular to each other. Data has been corrected to account for polarization dependence of the microscope and spectrograph. See section 11 in the ESI for details.

centrosymmetry. In addition to this, deterioration of the structure of MOF-177 when exposed to air has been reported previously.³⁸

In order to explore how SHG can be emitted from a centrosymmetric crystal, we have performed polarized SHG analysis under ambient conditions as reported by van der Veen *et al.*³⁹ By conducting a series of tests using a polarizer and an analyzer, the point group of a crystalline sample can be determined. The results can be seen in Figure 4. All tests showed zero symmetry axes and the SHG never vanished. Following the flow chart described by van der Veen *et al.*, it can be concluded that the point group of MOF-177 in this case is P1 pointing to a non-centrosymmetric triclinic crystal structure. A triclinic structure has been theoretically predicted previously after accommodation of C₆₀.²⁸ No other point groups could be detected for several crystals which is why we assume P1 is the dominant point group present in the sample. .

Our measurements suggest that removal from a solvent and exposure to air could already cause changes to the structure of MOF-177.

There are several possibilities that could explain the increase in SHG intensity in case of Li@C₆₀MOF-177: 1) the presence of a guest molecule itself, 2) structural changes (meaning change of point/space group) of the host and/or guest due to accommodation, 3) increased dipole moment due to interaction between host and guest.

Despite its centrosymmetry, bulk SHG emission from C₆₀ films has been reported and was attributed to magnetic dipole and electric quadrupole moments.^{40,41} This can explain the slight increase in emission for C₆₀MOF-177.

Seeing as C₆₀ is causing a slight increase in emission, it is likely that part of the larger increase in emission strength of Li@C₆₀MOF-177 is simply due to the presence of Li@C₆₀ as well as oDCB. It has been shown by Campbell *et al.* as well as our group that Li@C₆₀ has stronger NLO properties compared to ordinary C₆₀ and thus stronger emission from Li@C₆₀MOF-177

compared to C_{60} MOF-177 is expected.²¹⁻²³ However, there are more factors contributing to the overall increased emission.

Although change of the crystal structure of MOF-177 after accommodation of C_{60} has been predicted²⁸, in this case it does not seem to be associated with any meaningful increase in SHG intensity as it should cause measurable increases in both $Li@C_{60}$ MOF-177 and C_{60} MOF-177 and the crystal structure is the same for empty MOF-177 in our study. Small additional structural changes induced by $C_{60}/Li@C_{60}$ cannot be excluded by this study, however they do not seem to cause a noticeable change in NLO emission.

Furthermore, the interaction between Li^+ and the Zn-O bond of MOF-177 is causing tensile strain on the Zn-O bond. Increased length of the bond means an increased dipole moment if the charges remain the same. Such an increased dipole moment can further improve overall NLO emission.⁴²

Conclusions

We have shown how the NLO emission of MOF-177 can be significantly enhanced by accommodating $Li@C_{60}$ into the pores and how the interaction between the two is likely further increasing the emission properties. We have further shown that MOF-177 slightly deviates from the reported crystal structure when exposed to air as well as the stabilization of $Li@C_{60}$ by accommodation into the MOF.

By considering both host and guest for NLO emission, the overall signal can be greatly improved and the whole volume of the MOF, both the framework as well as the pores, are used efficiently for NLO. Additionally, due to the interaction between host and guest, the emission can be further strengthened. In the future, by carefully considering all factors highly efficient NLO active MOFs can be created: 1) choosing an NLO active host, 2) choosing an NLO active guest and 3) using interaction between host and guest to further enhance NLO properties. Using this holistic approach to MOF, their performance can be greatly improved. Furthermore, the approach can be potentially expanded to other organic porous materials as design flexibility is a common feature of organic materials.

Experimental

$Li^+@C_{60}(PF_6^-)$ powder that was purified through recrystallization was purchased from Idea International Co. Ltd.

Microcrystals of MOF-177 were synthesized according to the literature (J. Mater. Chem., 2007, 17, 3197–3204).

Introduction of C_{60} into MOFs: As-synthesized crystals were immersed into a saturated toluene solution of fullerene C_{60} (10 mL) at room temperature. The suspension was heated to 60 °C in an oven. After 1 day, the supernatant was removed by decantation, another 10 mL of saturated fullerene solution was added to the residue, and the resulting suspension was again allowed to stand at 60 °C. After 1 week with six solution-replacement cycles, the inclusion complex was obtained (Nat. Chem., 2010, 2, 780–783).

Introduction of $Li@C_{60}$: As-synthesized crystals were immersed into oDCB/ ACN solution of $Li^+@C_{60}(PF_6^-)$ (1 mg/mL) at room temperature. After 1 day, the supernatant was removed by decantation, another solution of $Li^+@C_{60}(PF_6^-)$ was added to the residue, and the resulting suspension was again allowed to stand at room temperature.

After soaking MOF-177 crystals in the solutions of C_{60} or $[Li^+@C_{60}]$, the residual C_{60} and $[Li^+@C_{60}]$ were repeatedly washed out with their solvents until the washouts become colorless. C_{60} MOF-177 and $Li@C_{60}$ MOF-177 are brown and dark brown, respectively (Figure S12).

ICP-OES: $Li@C_{60}$ MOF-177 was decomposed by HCl(aq) and neutralized by NaOH(aq). The resultant solution was mixed with acetonitrile to dissolve organic components. The final solution was analyzed by ICPE-9000, SHIMADZU CORPORATION.

Thermogravimetry of $[Li^+@C_{60}](PF_6^-)$, MOF-177 and $Li@C_{60}$ MOF-177 were carried out with Thermo plus EVO II TG8120 HUM-1F, Rigaku.

Raman spectroscopy: Raman spectra of microcrystals were obtained by inVia Reflex (Renishaw) with 785 nm laser. Measurements of peak position at 415 cm^{-1} were obtained with the same setup as describes under “NLO measurements” but with 633 nm excitation from a He-Ne laser and a 645 long-pass filter to block excitation light in front of the spectrograph.

NLO measurements have been performed on an inverted optical microscope (Ti-U, Nikon). The samples were illuminated by a femtosecond (fs) pulse at 820 nm (Mai Tai HP, Spectra-Physics, 120 fs, 80 MHz). The excitation beam was focused by an objective lens (10x Plan Fluor, NA 0.30, Nikon). The backscattered NLO signal was collected through the same objective. Spectra were recorded using a charge-coupled device (CCD) camera (DU920P, Andor) with a spectrograph (iHR320, Horiba). Out of focus signal was removed using a pinhole. Excitation light was blocked by a 750 short-pass filter (ET750sp, Chroma). Spectra were obtained from the central regions of MOFs. Integration time for every spectrum was 5 s. For each type of MOF (MOF-177 (toluene), MOF-177 (o-dichlorobenzene/acetonitrile), C_{60} MOF-177, $Li@C_{60}$ MOF-177) 40 spectra were recorded (20 for MOF-177 in o-dichlorobenzene/acetonitrile) and the average intensities calculated from these. Measurements were carried out under ambient conditions.

UV-vis measurement was carried out on a Lambda 950 (PerkinElmer) spectrophotometer using blank correction.

Conflicts of interest

There are no conflicts to declare.

Acknowledgements

This work was supported by Research Foundation – Flanders (FWO, G0D4519N, G081916N) and the KU Leuven Research Fund (C14/15/053, C14/19/079). M.W. acknowledges the FWO SB PhD fellowship (1S87920N). This collaborative work was partially supported by JSPS ‘Core-to-Core Program A. ‘Advanced Research Networks’ and JSPS Kakenhi (JP 20K21200, JP 21H01899, JP 21H04634, JP 20K21165, JP 19KK0136). The authors thank Dr. Kazuki Umemoto for providing C_{60} films.

Notes and references

- 1 H. K. Chae, D. Y. Siberio-Pérez, J. Kim, Y. Go, M. Eddaoudi, A. J. Matzger, M. O'Keeffe and O. M. Yaghi, *Nature*, 2004, **5**, 523-527
- 2 S. Kitagawa, R. Kitaura and S. Noro, *Angew. Chem. Int. Ed.*, 2004, **43**, 2334
- 3 J. Liu and C. Wöll, *Chem. Soc. Rev.*, 2017, **46**, 5730
- 4 N. Yanai, T. Uemura, M. Inoue, R. Matsuda, T. Fukushima, M. Tsujimoto, S. Isoda and S. Kitagawa, *J. Am. Chem. Soc.*, 2012, **134**, 4501
- 5 H. Li, M.M. Sadiq, K. Suzuki, R. Ricco, C. Doblin, A.J. Hill, S. Lim, P. Falcaro and M.R. Hill, *Adv. Mater.*, 2016, **28**, 1839
- 6 R. B. Lin, Z. J. Zhang and B. L. Chen, *Acc. Chem. Res.*, 2021, **54**, 3362
- 7 O. Shekhah, V. Chenikova, Y. Belmabkhout and M. Eddaoudi, *Crystals*, 2018, **8**, 412
- 8 H. Meng; C. Zhao, M. Nie, C. Wang and T. Wang, *J. Phys. Chem. C*, 2019, **123**, 6265
- 9 Y. Li, T. Wang, H. Meng, C. Zhao, M. Nie, L. Jiang and C. Wang, *Dalton Trans.*, 2016, **45**, 19226
- 10 D. S. Krylov, F. Liu, A. Brandenburg, L. Spree, V. Bon, S. Kaskel, A. U. B. Wolter, B. Büchner, S. M. Avdoshenko and A. A. Popov, *Phys. Chem. Chem. Phys.*, 2018, **20**, 11656
- 11 X. Huang, Q. Li, X. Xiao, S. Jia, Y. Li, Z. Duan, L. Bai, Z. Yuan, L. Li, Z. Lin and Y. Zhao, *Inorg. Chem.*, 2018, **57**, 6210
- 12 M. Liu, H. S. Quah, S. Wen, Z. Yu, J. J. Vittal and W. Ji, *Chem. Mater.*, 2016, **10**, 3385
- 13 R. Medihetty, J. K. Zareba, D. Mayer, M. Samoć and R. A. Fischer, *Chem. Soc. Rev.*, 2017, **46**, 4976
- 14 T. Popmintchev, M.-C. Chen, P. Arpin, M. M. Murnane and H. C. Kapteyn, *Nature Photon.*, 2010, **4**, 822
- 15 D. Cotter, R. J. Manning, K. J. Blow, A. D. Ellis, A. E. Kelly, D. Nesses, I. D. Phillips, A. J. Poustie and D. C. Rogers, *Science*, 1999, **286**, 1523
- 16 B. Gu, W. Yuan, M. H. Frosz, A. P. Zhang, S. He and O. Bang, *Opt. Lett.*, 2012, **37**, 794
- 17 F. Castet, V. Rodriguez, J.-L. Pozzo, L. Ducasse, A. Plaquet and B. Champagne, *Acc. Chem. Res.*, 2013, **46**, 2656
- 18 E. A. Migal, F. V. Potemkin and V. M. Gordienko, *Opt. Lett.*, 2017, **42**, 5218
- 19 D. N. Nikogosyan, *Nonlinear Optical Crystals: A Complete Survey*, Springer, New York, 2005
- 20 H. S. Nalwa, *Appl. Organomet. Chem.*, 1991, **5**, 349
- 21 M. Wolf, S. Toyouchi, P. Walke, K. Umemoto, A. Masuhara, H. Fukumura, Y. Takano, M. Yamada, K. Hirai, E. Fron and H. Uji-I, *RSC Adv.*, 2021, **12**, 389
- 22 E. E. B. Campbell, S. Couris, M. Fanti, E. Koudoumas, N. Kraewez and F. Zerbetto, *Adv. Mater.*, 1999, **11**, 405
- 23 E. E. B. Campbell, M. Fanti, I. V. Hertel, R. Mitzner and F. Zerbetto, *Chem. Phys. Lett.*, 1998, **288**, 131
- 24 Y. Inokuma, T. Arai and M. Fujita, *Nature Chem.*, 2010, **2**, 780
- 25 A. Saura-Sanmartin, A. Martinez-Cuezva, M. Marin-Luna, D. Bautista and J. Berna, *Angew. Chem. Int. Ed.*, 2021, **60**, 10814
- 26 V. Martinez, B. Karadeniz, N. Biliskov, I. Loncari, S. Muratovic, D. Zilic, S. M. Avdoshenko, M. Roslova, A. A. Popov and K. Uzarevic, *Chem. Mater.*, 2020, **32**, 10628
- 27 G. Xu, Z. Meng, X. Guo, H. Zhu, K. Deng, C. Xiao and Y. Liu, *Comp. Mater. Sci.*, 2019, **168**, 58
- 28 S. Aoyagi, E. Nishibori, H. Sawa, K. Sugimoto, M. Takata, Y. Miyata, R. Kitaura, H. Shinohara, H. Okada, T. Sakai, Y. Ono, K. Kawachi, K. Yokoo, S. Ono, K. Omote, Y. Kasama, S. Ishikawa, T. Komuro and H. Tobita, *Nature Chem.*, 2010, **2**, 678
- 29 Y. Morishige and A. Kimura, *SEI Tech. Rev.*, 2008, **66**, 106
- 30 S. S. Han, J. L. Mendoza-Cortés and W. A. Goddard III *Chem. Commun.*, 2014, **50**, 10994
- 31 V. N. Denisov, A. A. Zahkidov, R. Danieli, G. Ruani, R. Zamboni and C. Taliani, *Int. J. Mod. Phys. B*, 1992, **6**, 4019
- 32 M. K. Johnson, D. B. Powell and R. D. Cannon, *Spectrochimica Acta*, 1981, **10**, 899
- 33 D. Gültekin and H. Akbulut, *Acta Phys. Pol. A*, 2016, **129**, 803
- 34 D. Tuschel, *Spectroscopy*, 2019, **34**, 10
- 35 A. Kaphle, E. Echeverria, D. N. McIlroy, K. Roberts and P. Hari, *J. Nanosci. Nanotechnol.*, 2019, **19**, 3893
- 36 L. Popović, D. de Waal and J. C. A. Boeyens, *J. Raman. Spectrosc.*, 2005, **36**, 2
- 37 Y.-B. Zhang, H. Furukawa, N. Ko, W. Nie, H. J. Park, S. Okajima, K. E. Crodova, H. Deng, J. Kim and O. M. Yaghi, *J. Am. Chem. Soc.*, 2015, **137**, 2641
- 38 D. Saha and S. Deng, *J. Phys. Chem. Lett.*, 2010, **1**, 73
- 39 M. A. van der Veen, F. Vermoortele, D. E. De Vos and T. Verbiest, *Anal. Chem.*, 2012, **84**, 6378
- 40 X. K. Wang, T. G. Zhang, W. P. Lin, S. Z. Liu, G. K. Wong, M. M. Kappes, R. P. H. Chang and J. B. Ketterson, *Appl. Phys. Lett.*, 1992, **60**, 810.
- 41 Z. Shuai and J.-L. Brédas, *Adv. Mater.*, 1994, **6**, 6
- 42 M. Das, S. Rana and P. Sen, *J. Nonlinear Opt. Phys. Mater.*, 2010, **19**, 445